Discovery and Pharmacological Evaluation of a Novel Series of Adamantyl Cyanoguanidines as $P2X_7$ Receptor Antagonists

James O'Brien-Brown[1], Alexander Jackson[2], Tristan A. Reekie[1], Melissa L. Barron[3], Eryn L. Werry[3], Paolo Schiavini[1], Michelle McDonnell[2], Lenka Munoz[4], Shane Wilkinson[1], Benjamin Noll[5], Shudong Wang[5], and Michael Kassiou[1,#]

[1] School of Chemistry, The University of Sydney, NSW 2006 Australia

[2] School of Medical Sciences, The University of Sydney, NSW 2006 Australia

[3] Faculty of Health Sciences, The University of Sydney, NSW 2006 Australia

[4] Charles Perkins Centre, The University of Sydney, NSW 2006 Australia

[5] School of Pharmacy and Medical Sciences, University of South Australia, SA 5001 Australia

Corresponding Author

[#]E-mail: michael.kassiou@sydney.edu.au. Phone: +612 9351 2745

The authors declare no competing financial interest.

ABSTRACT: Here we report adamantyl cyanoguanidine compounds based on hybrids of the adamantyl amide scaffold reported by AstraZeneca and cyanoguanidine scaffold reported by Abbott Laboratories. Compound **27** displayed five-fold greater inhibitory potency than the lead compound **3** in both pore-formation and interleukin-1β release assays, while **35**-treated mice displayed an antidepressant phenotype in behavioral studies. This SAR study provides a proof of concept for hybrid compounds, which will help in the further development of $P2X_7R$ antagonists.

Keywords: $P2X_7R$ antagonist; P2X receptor; Adamantane; Inflammation; IL-1β; ATP

INTRODUCTION

The purinergic $P2X_7$ receptor ($P2X_7R$) is a ligand-gated ionotropic receptor activated by high concentrations of extracellular ATP. Activation of the $P2X_7R$ by ATP opens a pore allowing K^+ efflux associated with the processing and secretion of pro-inflammatory cytokines interleukin (IL)-1β and IL-18.[1-3] $P2X_7R$ is highly expressed on immune cells including microglia, the resident macrophages of the central nervous system (CNS). Secretion of IL-1β by activated microglia is linked to neurodegeneration associated with multiple sclerosis, Parkinson's, Alzheimer's, and Huntington's disease.[4-6] Patients with increased levels of inflammatory cytokines also exhibit behavioural patterns consistent with depressive mood disorders, and studies using $P2X_7R$-KO mice demonstrate an anti-depressant phenotype in animal models of stress.[7, 8] Given the role of $P2X_7R$ in inflammation, IL-1β processing and secretion, there has been a large focus on developing $P2X_7R$ antagonists for the treatment of neurodegenerative and psychiatric disorders.[9] Despite favourable preclinical evidence for the $P2X_7R$ as a drug target, there have been no $P2X_7R$ antagonists that have entered clinical trials for a CNS indication to date.[10] Additionally, the Pfizer drug CE-224,535 and AstraZeneca's AZD9056 both failed to display significant efficacy in phase II clinical trials for the treatment of a peripheral inflammatory disorder—rheumatoid arthritis.[11-13]

$P2X_7R$ antagonists featuring the polycyclic adamantyl moiety have been extensively studied. High potency and selectivity for the $P2X_7R$ subtype was reported for aryl carbohydrazides, adamantyl isoquinolinones, and adamantyl benzamides.[14-16] Inclusion of the adamantyl group increases blood-brain barrier penetration through optimization of lipophilic properties of polar compounds, and adamantane has proven to be one of the most potent hydrophobic groups in SAR studies of $P2X_7R$ antagonists.[17-19] Adamantyl amide derivatives incorporating substituted phenyl moieties are highly potent, but their poor pharmacokinetic properties preclude their use *in vivo*.[14, 15, 20, 21] However, the inclusion of a heterocyclic aryl group such as the indazole **1** reported by AstraZeneca (**Figure 1**) affords adamantyl amide derivatives which exhibit reduced intrinsic clearance (Cl_{int} = 47 mL/min/kg) and a reasonable half-life ($t_{1/2}$ = 1.0 h) in rats when compared to the corresponding phenyl analogues.[14]

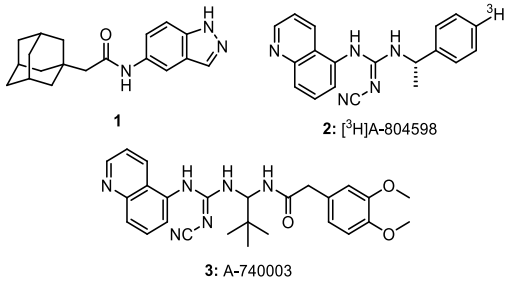

Figure 1. The adamantyl indazole amide **1** reported by AstraZeneca, and the cyanoguanidine derivatives **2**–**3** developed by Abbott Laboratories.

An alternative class of $P2X_7R$ antagonists developed by Abbott Laboratories incorporates a cyanoguanidine motif. These compounds demonstrate potent and selective $P2X_7R$ inhibition with minimal difference in activity across species.[22] Compound **3** (A-740003) inhibited *in*

vitro human $P2X_7R$ activity with IC_{50} values ranging from 44–155 nM for IL-1β release, calcium flux, and YO-PRO®-1 dye uptake assays.[22] More recently, the truncated analogue **2** (A-804598) was reported with an IC_{50} of 9–11 nM at the mouse, rat, and human $P2X_7Rs$ in a calcium flux assay, with comparable potencies also observed in IL-1β release and YO-PRO®-1 dye uptake assays.[23] These cyanoguanidine derivatives exhibit acceptable pharmacokinetic properties that have allowed for their use *in vivo*, and the high potency and selectivity of **2** for the $P2X_7R$ over other P2X receptors has led to the use of [^{3}H]A-804598 as a high affinity radioligand in rat $P2X_7R$ binding studies.[23]

To retain the favourable pharmacokinetic properties of the truncated cyanoguanidines reported by Abbott Laboratories, but produce enhanced potency by the inclusion of the adamantyl moiety, in this work we describe an exploratory SAR study of adamantyl-cyanoguanidine hybrid compounds **4** (**Figure 2**). They incorporate adamantane (pink) as the hydrophobic portion of the molecule connected to variously substituted aryl groups (green) through the cyanoguanidine linker (red). We investigated the optimal distance of the cyanoguanidine linker to the adamantyl (L_1 = 0–2, orange) and aryl (L_2 = 0–2, blue) groups. These compounds were investigated as a proof-of-concept for establishing whether two distinct, promising classes of $P2X_7R$ antagonists can be combined to form hybrid molecules which retain desirable features from each category to further explore the pharmacophore of $P2X_7R$ inhibition.

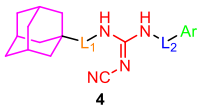

4

Figure 2. Adamantyl-cyanoguanidine hybrids investigated for their potency of inhibition at the human $P2X_7R$.

RESULTS AND DISCUSSION

Chemistry. Phenyl *N*-adamantyl *N*'-cyanocarbamimidate **6** was prepared from the corresponding adamantyl amine **5** and the commercially available diphenyl *N*-cyanocarbonimidate in 2-propanol (**Scheme 1**). Subsequent reaction of **6** with commercially available aryl amines, followed by removal of solvent *in vacuo* and trituration with diethyl ether yielded *N*-adamantyl-*N*'-cyanoguanidines of type **7**, with high purity for *in vitro* analysis. For less nucleophilic aryl amines, such as 5-aminoquinoline, it was necessary to couple the aryl portion **8** with diphenyl *N*-cyanocarbonimidate first to give **9**, followed by the reaction with adamantyl amine **5** to yield *N*-adamantyl-*N*'-cyanoguanidines of type **7**.

$P2X_7R$ Inhibition Assay. The adamantyl cyanoguanidine compounds **10–36** were assayed for inhibition of $P2X_7R$ activity by measuring the inhibition of 2′(3′)-*O*-(4-benzoylbenzoyl) ATP (BzATP)-induced uptake of YO-PRO®-1 dye in human THP-1 cells (**Tables 1, 2** and **3**). Further experimental details are provided in the supporting information.

Scheme 1. Synthesis of adamantyl cyanoguanidine derivatives

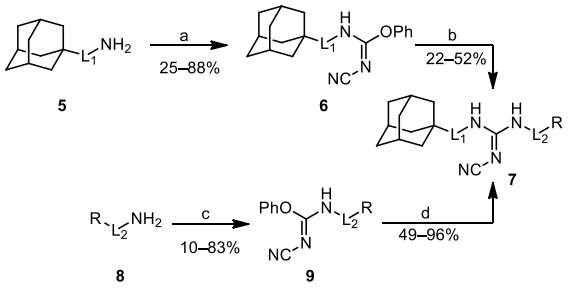

[a] Reagents and conditions: (a) diphenyl *N*-cyanocarbonimidate, *i*-PrOH, 22 °C; (b) aryl amine, *i*-PrOH or *i*-PrOH/EtOAc/CH_2Cl_2, reflux; (c) diphenyl *N*-cyanocarbonimidate, MeCN, reflux; (d) adamantyl amine **5**, *i*-PrOH, reflux.

The effects of the linker length of both the adamantyl (L_1) and aryl portion (L_2) of the molecule were explored whilst retaining the unsubstituted phenyl ring (**Table 1**). Exploring linker L_1 showed that compounds **10**–**12** (L_1 = 0) were all weakly potent with a maximum potency of ~2.5 μM, while the ethylene linker ($L_1 = (CH_2)_2$, **16**–**17**) was also poorly tolerated, only yielding high micromolar potency.

Table 1. The IC_{50} values of adamantyl cyanoguanidine derivatives against hP2X$_7$R using the YO-PRO®-1 dye uptake functional assay in human THP-1 cells.

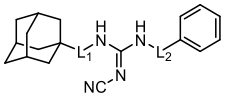

compound	L_1	L_2	IC_{50} (dye uptake) mean ± SEM (nM)[a]
10	-	-	2455 ± 57
11	-	$–CH_2–$	>10000
12	-	$–(CH_2)_2–$	>10000
13	$–CH_2–$	-	100 ± 5
14	$–CH_2–$	$–CH_2–$	407 ± 28
15	$–CH_2–$	$–(CH_2)_2–$	4070 ± 380
16	$–(CH_2)_2–$	-	>10000
17	$–(CH_2)_2–$	$–CH_2–$	3020 ± 350

[a] IC_{50} values are the mean of three experiments, with the uncertainty reported as the standard error of the mean.

The methylene linker ($L_1 = CH_2$) proved to be ideal for the adamantyl portion of the molecule (compounds **13**–**15**), with sub-micromolar potency achieved for **13** and **14** (100 and 407 nM, respectively). In comparison, greater tolerance was observed for the aryl linker (L_2). Compounds **13** and **14** showed that no linker (L_2 = 0), or a methylene linker ($L_2 = CH_2$) afforded reasonable potency in combination with the preferred adamantylmethyl ($L_1 = CH_2$) substituent. Extending the linker further (**15**, $L_2 = (CH_2)_2$) was poorly tolerated, with potency decreasing 10-fold (4070 nM) compared to the methylene linker. Following identification of the optimal L_1 and L_2 linker lengths, further studies were conducted on the aromatic portion of the molecule to explore the effect of aryl substitution on antagonist potency (**Table 2**).

The effect of electron-donating, electron-withdrawing, and heteroaromatic aryl derivatives were tested while varying the L_2 linker length to determine if the directly attached (L_2 = 0) anilide-like derivatives were still superior to the methylene linker when the ring substitutions were altered. First examining when no linker was present (L_2 = 0), the addition of an electron-donating methoxy substituent in positions 2 (**18**) and 3 (**19**) gave compounds which were twice as potent as the unsubstituted analogue **13** (51 and 58 nM vs 100 nM, respectively). The 4-methoxy derivative **20** was an order of magnitude less potent (562 nM) than the other methoxy regioisomers with a five-fold reduction in potency compared to **13**. Addition of an electron-withdrawing fluoro substituent in positions 3 and 4 (compounds **22**–**23**) gave compounds of slightly reduced potency (186 and 174 nM, respectively) compared to **13**, while the 2-fluoro analogue **21** displayed similar potency (58 nM) to the 2- and 3-methoxy analogues (**18** and **19** respectively). The pyridyl derivatives **24**–**26** were all less potent than **13**, with the 2-pyridyl analogue **24** showing a complete loss of activity (*cf.* 214 and 417 nM for **25** and **26**, respectively). The high potency of the *ortho*-substituted (L_2 = 0) derivatives may be due to a steric clash with the cyanoguanidine linker, leading to a twisted conformation of the aryl ring which interacts more favourably with residues in the active site, as has been suggested for 2-substituted benzamide derivatives.[14]

With the extended methylene (L_2 = CH_2) linker, both electron-donating methoxy derivatives (**28**–**30**; 562, 851 and >10000 nM) and electron-withdrawing fluoro derivatives (**31**–**33**; 501, 708 and 2399 nM) were at least an order of magnitude less potent than the directly attached (L_2 = 0) analogues. Interestingly, there was a reversal in activity for the heteroaromatic derivatives (**34**–**36**), exhibiting equivalent (4-pyridyl; 447 vs 417 nM) or higher (2- and 3-pyridyl; 234 vs >10000 nM, and 69 vs 214 nM) potency with the methylene linker (L_2 = CH_2) than for the directly attached (L_2 = 0) pyridines. The substantial potency increase observed in the 2-pyridyl derivative with the methylene linker **34** compared to **24** (L_2 = 0) may potentially result from **24** favouring inactive tautomers (**24a** and **24b**) which benefit from an intramolecular hydrogen-bonding interaction (**Figure 3**), which is not possible with the alternative regiomeric pyridines (see supporting information for further conformational analysis of selected cyanoguanidine compounds).

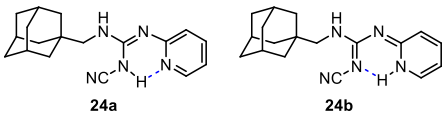

Figure 3. Potential tautomers of **24** resulting from the energetically favourable intramolecular hydrogen-bonding interactions.

Table 2. The IC_{50} values of adamantyl cyanoguanidine derivatives with varying aryl groups.

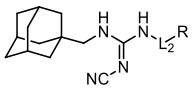

Compound	L_2	R	IC_{50} (dye uptake) mean ± SEM (nM)[a]	cLogP[b]	LiPE[c]
18	-	2-CH_3O-C_6H_4	51 ± 5	4.48	2.81
19	-	3-CH_3O-C_6H_4	58 ± 3	4.48	2.76
20	-	4-CH_3O-C_6H_4	562 ± 39	4.48	1.77
21	-	2-F-C_6H_4	58 ± 1	4.76	2.48
22	-	3-F-C_6H_4	186 ± 13	4.76	1.97
23	-	4-F-C_6H_4	174 ± 8	4.76	2.00
24	-	2-pyridyl	>10000	3.98	N/A
25	-	3-pyridyl	214 ± 5	3.27	3.40
26	-	4-pyridyl	417 ± 38	3.27	3.11
27	-	5-quinolinyl	18 ± 2	4.69	3.06
28	–CH_2–	2-CH_3O-C_6H_4	562 ± 26	4.69	1.56
29	–CH_2–	3-CH_3O-C_6H_4	851 ± 20	4.69	1.38
30	–CH_2–	4-CH_3O-C_6H_4	>10000	4.69	N/A
31	–CH_2–	2-F-C_6H_4	501 ± 81	4.97	1.33
32	–CH_2–	3-F-C_6H_4	708 ± 33	4.97	1.18
33	–CH_2–	4-F-C_6H_4	2399 ± 277	4.97	0.65
34	–CH_2–	2-pyridyl	234 ± 22	3.90	2.73
35	–CH_2–	3-pyridyl	69 ± 3	3.48	3.68
36	–CH_2–	4-pyridyl	447 ± 10	3.48	2.87

[a] IC_{50} values are the mean of three experiments, with the uncertainty reported as the standard error of the mean. [b] Calculated in ChemDraw Ultra v. 12.0.2 using Crippen's fragmentation method. [c] Lipophilic efficiency: LiPE = pIC_{50} – cLogP.

The 5-quinolinyl **27**, which is the adamantylmethyl analogue of **3** was found to be more potent than any of the compounds tested (18 nM), with five times higher potency than **3** in both the dye uptake and IL-1β release assays (**Table 3**).[23] An interesting feature of the 5-quinoline is the equivalent nitrogen positioning to that of the most potent regiomeric pyridine **35** (**Figure 4**). This increase in potency compared to the pyridine might be due to the rigidification of the methylene linker with the bioisosteric quinoline, resulting in a more favourable restricted conformation in the binding site. Alternatively, the phenyl portion of quinoline may result in increased potency through cation-π interactions with a positively charged amino acid residue, as well as acting as a hydrogen-bond acceptor through the nitrogen atom in the adjoined fused ring.

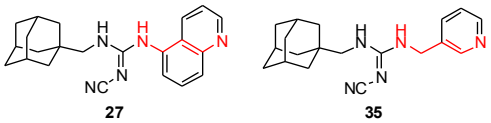

27 **35**

Figure 4. The equivalent nitrogen positioning of the 5-quinolinyl and 3-pyridyl derivatives.

An IL-1β release assay was performed on selected compounds to validate the results obtained from the dye uptake assay (**Table 3**). The IC_{50} values from the IL-1β assay showed consistently stronger potency than the IC_{50} values for dye uptake across all compounds tested. An interesting observation can be made wherein the quinoline derivatives (**3** and **27**) exhibited a ~10-fold increase in potency when tested in the IL-1β release assay, the phenyl derivatives (**14** and **32**) showed a ~5-fold increase in activity, and the pyridyl derivatives (**34**–**36**) all demonstrated a ~1.5-fold increase in activity. While the sample set is small, the consistency of the *n*-fold potency increase suggests that the nature of the aromatic group is a determining factor in the apparent potency increase observed when tested with the IL-1β release assay. The IL-1β assay is conducted with preincubation of the antagonist compounds, followed by a wash step. Compounds with the more lipophilic aromatic systems tend to exhibit the highest increase in IC_{50} with the IL-1β assay, potentially due to cell permeability effects, or by having a slow rate of dissociation (k_{off}) from the receptor. Slowly dissociating antagonist compounds give a higher receptor occupancy due to their increased residence time, so the wash step which effectively removes any unbound ligand will favour slowly dissociating compounds.[24-26]

Table 3. IC_{50} values of adamantyl cyanoguanidine derivatives in both YO-PRO-1® dye uptake and IL-1β release assays.

Number	Compound	IC_{50} (dye uptake) mean ± SEM (nM)[a]	IC_{50} (IL-1β) mean ± SEM (nM)[a]	*n*-fold increase in activity (dye uptake/IL-1β release)
3	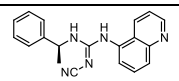	93 ± 2	9 ± 2	10.3
27	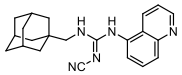	18 ± 2	2 ± 1	9.0
14	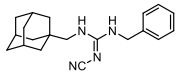	407 ± 28	79 ± 17	5.2
32	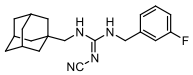	708 ± 33	132 ± 6	5.4
34	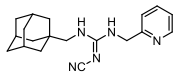	234 ± 22	138 ± 3	1.7
35	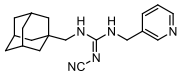	69 ± 3	40 ± 4	1.7
36	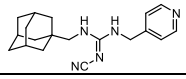	447 ± 10	389 ± 27	1.2

[a] IC_{50} values are the mean of three experiments.

Despite the higher potency of the quinoline **27**, the lower calculated logP of the 3-pyridyl derivative **35** yielded a compound with a higher LiPE value than the quinoline, suggesting that it was likely to be a better 'drug-like' candidate based on its calculated physicochemical properties. Furthermore, the calculated pharmacokinetic properties of **35** were predominantly within the recommended values as suggested by Schrödinger, and with similar values to 95% of known drugs (**Table 4**). Due to the combination of desirable *in silico* physicochemical and pharmacokinetic properties, **35** was chosen as an illustrative compound from the adamantyl cyanoguanidine series for further *in vivo* biological studies.[27] *In vivo* pharmacokinetic

studies were conducted in mice with **35** administered intravenously as a bolus dose (2 mg/kg), with further details provided in the supporting information. The compound was rapidly cleared (Cl = 117 mL/min·kg), had a short half-life ($t_{1/2}$ = 0.22 h), and a low overall exposure ($AUC_{0–\infty}$ = 0.88 μM·h). Despite the far from ideal pharmacokinetic properties of **35**, compounds with short half-lives are still able to display activity through the forced-swim test (FST) as a result of the short duration of the procedure (6 min).[28, 29] While the pharmacokinetic profile of **35** would make it unsuitable for clinical development, and is by no means a viable lead candidate itself, we believe it is sufficient for proof-of-concept studies in the FST.

Table 4. Calculated physicochemical and pharmacokinetic properties, and *in vivo* pharmacokinetics of 35.

Calculated properties	**MW** (g/mol)[a]	**log P**[a]	**PSA** (Å^2)[a]	**Oral Absorption** (%)[b]	**QPPCaco** (nm/sec)[b]	**QPPMDCK** (nm/sec)[b]	**QPlogBB**[b]
	Recommended Values			Range for 95% of known drugs (Schrödinger)			
	< 450	< 5	< 70	< 25% poor > 80% high	< 25 poor > 500 great	< 25 poor > 500 great	–3.0 to –1.2
35	323.44	3.41	78.33	100	839	409	–0.905
Experimental pharmacokinetics[c]	**C_{max}** (μM)	**T_{max}** (min)	**$t_{1/2}$** (h)	**$AUC_{0-\infty}$** (μM·h)	**$MRT_{0-\infty}$** (h)	**Cl** (mL/min·kg)	**V_d** (mL/kg)
35	3.65	2.5	0.22	0.88	0.31	117	2202

[a] Physicochemical properties (molecular weight, MW; lipophilicity, log P; polar surface area, PSA) were calculated with ACD/Lab v12 software. [b] Pharmacokinetic properties (Oral Absorption; Predicted Apparent Caco-2 Permeability, QPPCaco; Predicted apparent MDCK cell permeability, QPPMDCK; Predicted Brain/Blood Partition Coefficient, QPlogBB) were calculated with QikProp, Schrödinger v4 software. [c] Pharmacokinetic parameters of 35 in mice after 2 mg/kg IV dose. Further details are provided in the supporting information.

To examine whether these compounds could penetrate the BBB, act on centrally expressed $P2X_7$Rs and induce a behavioural response *in vivo*, the 3-pyridyl analogue **35** (highest LiPE value; **Table 2**) was tested in the FST. The FST is a model of behavioural despair in mice. Immobility time in the FST is considered a reliable indicator of depressive activity as mice stop engaging in escape-oriented behaviour when placed in an inescapable environment, hence the FST is a commonly used paradigm for testing the efficacy of antidepressant drugs.[30, 31] In addition, previous studies have demonstrated that $P2X_7$R-KO mice display decreased immobility time compared to wild-type mice, validating the use of the FST as a model for $P2X_7$R antagonism in the CNS.[7] After intraperitoneal administration of vehicle or **35**, the tests were conducted by placing mice in a clear Plexiglas® cylinder filled with water, with the immobility time being defined as the time in seconds in which the mouse was passively floating in the chamber. Further experimental details are included in the supporting information. $P2X_7$R-KO mice and mice treated with analogue **35** showed reduced immobility time when compared to wild-type (WT) mice (**Figure 4**).

One-way repeated measures ANOVA on the third day of testing revealed that $P2X_7$R-KO mice displayed a significantly reduced immobility time compared to WT mice [$F(1,31)$ = 24.04, $P < 0.05$], while **35**-treated mice revealed a treatment by time interaction wherein they

behaved similarly to vehicle-treated mice in the first three minutes of the test, but showed a significant decrease in immobility time in the final three minutes of the test [$F(5,115) = 3.45$, $P < 0.01$]. These data are consistent with an anti-depressant phenotype as the induced behavioural despair response has diminished. These data provide evidence to suggest that **35** is able to act centrally and produce comparable reduction in depressive symptoms as genetic knock-down of the $P2X_7R$, presumably through $P2X_7R$-mediated inhibition of IL-1β release.[30, 32]

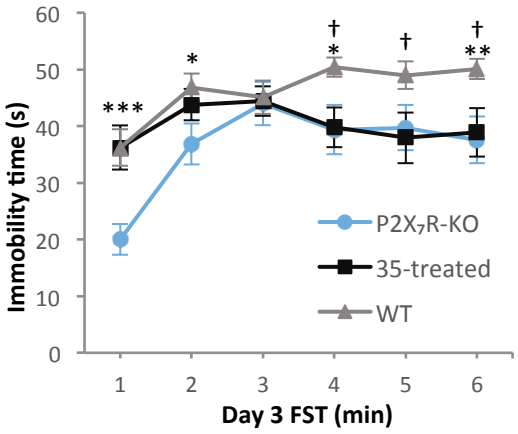

Figure 4. The immobility time of mice as a function of time in vehicle-treated $P2X_7R$-KO (n = 18), vehicle-treated WT (n = 15) and **35**-treated WT (1 mg/kg; n = 15) mice on Day 3 of consecutive daily repeated forced swim tests. Data are expressed as the mean ± SEM. Significant genotype effects per minute are indicated by * $P < 0.05$, ** $P < 0.01$, *** $P < 0.001$, and significant treatment effects per minute indicated by † $P < 0.05$, which were analysed using Student's *t*-test.

CONCLUSION

In summary, we demonstrate that the adamantyl moiety is an effective bioisostere for the hydrophobic aryl portion of the cyanoguanidine scaffold in $P2X_7R$ antagonists. The SAR study revealed features of this compound series required for $P2X_7R$ inhibition. The methylene linker to adamantane is essential for high inhibitory activity, while the aryl portion benefits from direct attachment ($L_2 = 0$) of the guanidino nitrogen for benzene derivatives. Interestingly a methylene linker ($L_2 = CH_2$) is more favourable for heteroaromatic analogues, which we have suggested to result from directly attached ($L_2 = 0$) electron deficient pyridyl analogues being unable to effectively participate in cation-π interactions in the active site. The adamantane analogue **27** is highly potent in both functional assays, displaying approximately 5-fold greater inhibitory activity than the lead compound **3**. Compound **35** demonstrated the ability to act centrally to produce an anti-depressant phenotype in the FST. The high potency and promising *in vivo* results for the adamantyl-cyanoguanidine compounds imply great potential for developing an effective CNS-penetrant $P2X_7R$ antagonist, and the SAR studies reported here will help guide the design of additional analogues which retain or improve upon the potency of **35**, with enhanced pharmacokinetic properties.

Supporting Information

Full synthetic details, and experimental protocols for biological assays are listed in the supporting information.

ACKNOWLEDGEMENTS

Work performed was supported by the NHMRC and in part by the European Union's Seventh Framework Programme [FP7/2007-2013] INMiND (Grant agreement No. HEALTH-F2-2011-278850).

ABBREVIATIONS USED

BzATP, 2'(3')-*O*-(4-Benzoylbenzoyl)adenosine-5'-triphosphate tri(triethylammonium) salt; DMSO, Dimethyl sulfoxide; FBS, Fetal bovine serum; HBSS, Hanks' Balanced Salt Solution; rhIFN-γ, Recombinant human interferon gamma; LPS, Lipopolysaccharide

REFERENCES

[1] L. Franchi, T. Eigenbrod, R. Munoz-Planillo, G. Nunez, The inflammasome: a caspase-1-activation platform that regulates immune responses and disease pathogenesis, Nat Immunol, 10 (2009) 241-247.

[2] P. Pelegrin, A. Surprenant, The P2X(7) receptor-pannexin connection to dye uptake and IL-1beta release, Purinergic signalling, 5 (2009) 129-137.

[3] Y. Chakfe, R. Seguin, J.P. Antel, C. Morissette, D. Malo, D. Henderson, P. Séguéla, ADP and AMP Induce Interleukin-1β Release from Microglial Cells through Activation of ATP-Primed P2X7 Receptor Channels, The Journal of Neuroscience, 22 (2002) 3061-3069.

[4] L.K. Parvathenani, S. Tertyshnikova, C.R. Greco, S.B. Roberts, B. Robertson, R. Posmantur, P2X7 mediates superoxide production in primary microglia and is up-regulated in a transgenic mouse model of Alzheimer's disease, The Journal of biological chemistry, 278 (2003) 13309-13317.

[5] P.L. McGeer, E.G. McGeer, The inflammatory response system of brain: implications for therapy of Alzheimer and other neurodegenerative diseases, Brain research. Brain research reviews, 21 (1995) 195-218.

[6] R. Le Feuvre, D. Brough, N. Rothwell, Extracellular ATP and P2X7 receptors in neurodegeneration, European Journal of Pharmacology, 447 (2002) 261-269.

[7] A.A. Boucher, J.C. Arnold, G.E. Hunt, A. Spiro, J. Spencer, C. Brown, I.S. McGregor, M.R. Bennett, M. Kassiou, Neuroscience, 189 (2011) 170.

[8] S. Velasquez, J. Rappaport, Inflammasome activation in major depressive disorder: A pivotal linkage between psychological stress, purinergic signaling, and the kynurenine pathway, Biol. Psychiatry, 80 (2016) 4–5.

[9] C.C. Chrovian, J.C. Rech, A. Bhattacharya, M.A. Letavic, P2X7 antagonists as potential therapeutic agents for the treatment of CNS disorders, Progress in medicinal chemistry, 53 (2014) 65-100.

[10] A. Bhattacharya, K. Biber, The microglial ATP-gated ion channel P2X7 as a CNS drug target, Glia, 64 (2016) 1772–1787.

[11] T.C. Stock, B.J. Bloom, N. Wei, S. Ishaq, W. Park, X. Wang, P. Gupta, C.A. Mebus, Efficacy and safety of CE-224,535, an antagonist of P2X7 receptor, in treatment of patients with rheumatoid arthritis inadequately controlled by methotrexate, J. Rheumatol., 39 (2012) 720–727.

[12] E.C. Keystone, M.M. Wang, M. Layton, S. Hollis, I.B. McInnes, Clinical evaluation of the efficacy of the P2X7 purinergic receptor antagonist AZD9056 on the signs and symptoms of rheumatoid arthritis in patients with active disease despite treatment with methotrexate or sulphasalazine, Ann. Rheum. Dis., 71 (2012) 1630–1635.
[13] R. Bartlett, L. Stokes, R. Sluyter, The P2X7 Receptor Channel: Recent Developments and the Use of P2X7 Antagonists in Models of Disease, Pharmacol. Rev., 66 (2014) 638–675.
[14] A. Baxter, J. Bent, K. Bowers, M. Braddock, S. Brough, M. Fagura, M. Lawson, T. McInally, M. Mortimore, M. Robertson, R. Weaver, P. Webborn, Hit-to-Lead studies: The discovery of potent adamantane amide P2X7 receptor antagonists, Bioorganic & medicinal chemistry letters, 13 (2003) 4047-4050.
[15] D.W. Nelson, K. Sarris, D.M. Kalvin, M.T. Namovic, G. Grayson, D.L. Donnelly-Roberts, R. Harris, P. Honore, M.F. Jarvis, C.R. Faltynek, W.A. Carroll, Structure-activity relationship studies on N'-aryl carbohydrazide P2X7 antagonists, J Med Chem, 51 (2008) 3030-3034.
[16] M.G. Kelly, J. Kincaid, Y. Fang, Y. Cao, C. Kaub, S. Gowlugari, Z. Wang, Bicycloheteroaryl compounds as P2X7 modulators and uses thereof, in, Google Patents, 2012.
[17] N. Tsuzuki, T. Hama, T. Hibi, R. Konishi, S. Futaki, K. Kitagawa, Adamantane as a brain-directed drug carrier for poorly absorbed drug: Antinociceptive effects of [D-Ala2] Leu-enkephalin derivatives conjugated with the 1-adamantane moiety, Biochemical Pharmacology, 41 (1991) R5-R8.
[18] N. Tsuzuki, T. Hama, M. Kawada, A. Hasui, R. Konishi, S. Shiwa, Y. Ochi, S. Futaki, K. Kitagawa, Adamantane as a brain-directed drug carrier for poorly absorbed drug. 2. AZT derivatives conjugated with the 1-adamantane moiety, Journal of pharmaceutical sciences, 83 (1994) 481-484.
[19] J. Liu, D. Obando, V. Liao, T. Lifa, R. Codd, The many faces of the adamantyl group in drug design, European journal of medicinal chemistry, 46 (2011) 1949-1963.
[20] S.M. Wilkinson, H. Gunosewoyo, M.L. Barron, A. Boucher, M. McDonnell, P. Turner, D.E. Morrison, M.R. Bennett, I.S. McGregor, L.M. Rendina, M. Kassiou, The First CNS-Active Carborane: A Novel P2X7 Receptor Antagonist with Antidepressant Activity, ACS Chemical Neuroscience, 5 (2014) 335-339.
[21] H. Gunosewoyo, J.L. Guo, M.R. Bennett, M.J. Coster, M. Kassiou, Cubyl amides: novel P2X7 receptor antagonists, Bioorganic & medicinal chemistry letters, 18 (2008) 3720-3723.
[22] P. Honore, D. Donnelly-Roberts, M.T. Namovic, G. Hsieh, C.Z. Zhu, J.P. Mikusa, G. Hernandez, C. Zhong, D.M. Gauvin, P. Chandran, R. Harris, A.P. Medrano, W. Carroll, K. Marsh, J.P. Sullivan, C.R. Faltynek, M.F. Jarvis, A-740003 [N-(1-{[(Cyanoimino)(5-quinolinylamino) methyl]amino}-2,2-dimethylpropyl)-2-(3,4-dimethoxyphenyl)acetamide], a Novel and Selective P2X7 Receptor Antagonist, Dose-Dependently Reduces Neuropathic Pain in the Rat, Journal of Pharmacology and Experimental Therapeutics, 319 (2006) 1376-1385.
[23] D.L. Donnelly-Roberts, M.T. Namovic, B. Surber, S.X. Vaidyanathan, A. Perez-Medrano, Y. Wang, W.A. Carroll, M.F. Jarvis, [3H]A-804598 ([3H]2-cyano-1-[(1S)-1-phenylethyl]-3-quinolin-5-ylguanidine) is a novel, potent, and selective antagonist radioligand for P2X7 receptors, Neuropharmacology, 56 (2009) 223-229.
[24] S. Núñez, J. Venhorst, C.G. Kruse, Target–drug interactions: first principles and their application to drug discovery, Drug Discov. Today, 17 (2012) 10–22.

[25] S. Kapur, P. Seeman, Antipsychotic agents differ in how fast they come off the dopamine D2 receptors. Implications for atypical antipsychotic action, J. Psychiatry Neurosci., 25 (2000) 161–166.
[26] G. Tresadern, J.M. Bartolome, G.J. Macdonald, X. Langlois, Molecular properties affecting fast dissociation from the D2 receptor, Bioorg. Med. Chem. Lett., 19 (2011) 2231–2241.
[27] P.D. Leeson, B. Springthorpe, Nat. Rev. Drug Discovery, 6 (2007) 881.
[28] B.J. Caldarone, D. Wang, N.E. Paterson, M. Manzano, A. Fedolak, K. Cavino, M. Kwan, T. Hanania, S.K. Chellappan, A.P. Kozikowski, B. Olivier, M.R. Picciotto, A. Ghavami, Dissociation between duration of action in the forced swim test in mice and nicotinic acetylcholine receptor occupancy with sazetidine, varenicline, and 5-I-A85380, Psychopharmacology (Berl.), 217 (2011) 199–210.
[29] K. Suemaru, K. Yasuda, R. Cui, B. Li, K. Umeda, M. Amano, H. Mitsuhashi, N. Takeuchi, T. Inoue, Y. Gomita, H. Araki, Antidepressant-like action of nicotine in forced swimming test and brain serotonin in mice, Physiol. Behav., 88 (2006) 545–549.
[30] R.D. Porsolt, A. Bertin, M. Jalfre, Behavioral despair in mice: a primary screening test for antidepressants, Archives internationales de pharmacodynamie et de therapie, 229 (1977) 327-336.
[31] R.D. Porsolt, G. Brossard, C. Hautbois, S. Roux, Rodent models of depression: forced swimming and tail suspension behavioral despair tests in rats and mice, Curr. Protoc. Neurosci., Chapter 8 (2001) Unit 8.10A.
[32] A.M. Basso, N.A. Bratcher, R.R. Harris, M.F. Jarvis, M.W. Decker, L.E. Rueter, Behavioral profile of P2X7 receptor knockout mice in animal models of depression and anxiety: Relevance for neuropsychiatric disorders, Behavioural Brain Research, 198 (2009) 83-90.